

Methodology for Zero-moment Point Experimental Modeling in the Frequency Domain

RONY CABALLERO

Technological University of Panama, Apartado Postal 0819-07289, El Dorado, Panama City, Panama

MANUEL A. ARMADA

PEDRO ALARCÓN

Automatic Control Department, Industrial Automation Institute – CSIC, 28500 La Poveda, Madrid, Spain (armada@iai.csic.es)

(Received 31 January 2006; accepted 17 May 2006)

Abstract: Frequency domain methodology is applied to obtain a nominal model for the Zero-Moment Point (ZMP) stability index of a biped robot in an attempt to establish a relationship between the robot trunk trajectories and the stability margin of the contact surface of the foot (or feet) touching the supporting soil. To this end the biped robot trunk is excited with a variable frequency sinusoidal signal around several operating points. These input oscillations generate other output oscillations that can be analyzed with the help of the ZMP measurement system. The proposed ZMP modeling approach not only considers classical rigid body model uncertainties but also non-modelled robot mechanical structure vibration modes. The non-linear ZMP model is obtained following three consecutive stages: Equivalent inverted pendulum dynamics, where saturation and acceleration upper bounds are taken into account, non-modelled inverted pendulum dynamics, including non-linear effects, and low-pass dynamics defining the system cut-off frequency. The effectiveness of this method is demonstrated in practice with the SILO2 biped robot prototype, and a simple control strategy is implemented in order to validate experimentally the usefulness of the models developed.

Key words: Legged locomotion, zero-moment point, frequency domain modeling, biped robot, stability

1. INTRODUCTION

Interest in legged robots is growing, both because of the inherent scientific challenge and as a result of their potential applications (Armada and González de Santos, 1997; Armada et al., 2003). Nevertheless, significant research effort is still required to simplify their inherent complexity (in both design and control) in order to advance towards the target of making them of real, practical usability (González de Santos et al., 2000; Virk et al., 2004; González de Santos et al., 2005).

Among legged robots, the possibility of using two-legged humanoid robots in practical applications is becoming more feasible, and important work dealing with design and control aspects of humanoid machines has now been realised (Hirai, 1999). One fundamental aspect of humanoid robot research that draws considerable attention from the scientific community is the stability problem of biped locomotion, and relevant contributions on this subject have

been put forward by many authors (Vukobratovic and Juricic, 1968; Furushu and Masubushi, 1986; Hemami et al., 1973; Mita et al., 1984; Yamaguchi et al., 1993; Goswami, 1999).

The alternation of single and double support phases during the locomotion cycle of a biped robot results in a complex robot-ground interaction (Fujimoto et al., 1998). This situation poses well known difficulties in the design of the control system for these machines and justifies the devotion of special attention to making the desired locomotion cycle possible. As a consequence, this has been an important research area for many scientists in recent years. Due to the fact that biped machines are so complex, most of these control designs involve the use of simplified dynamical modeling (Hemami, 1976). Nevertheless, biped robots are not only modelled assuming rigid links and ideal torque sources, but also presuppose sagittal and lateral plane dynamic decoupling (Medrano-Cerda and Eldukhri, 1997).

Although it is understandable that these simplifications are important for easing control architecture design and real-time motion planning, the use of an oversimplified model in presence of non-modelled structural elastic modes and non-modelled joint mechanical backlash could compromise the desired foot-ground stability. One of the most effective ways to analyze the foot-ground stability of biped robots is the so called zero moment point (ZMP), introduced in the pioneering work of Vukobratovic and his co-workers (Vukobratovic et al., 1968) as an index of stability for the walking cycle. The ZMP concept has been used successfully by many authors for biped robot trajectory selection (Yamaguchi et al., 1993; Hirai et al., 1998; Gienger et al., 1999; Pfeiffer et al., 2000).

In this article, a frequency domain response methodology is proposed for ZMP modeling. The proposed modeling methodology divides the ZMP dynamical model into three parts. The first corresponds to equivalent inverted pendulum dynamics, the second concerns low pass dynamics, and the third involves model uncertainty due to unmodelled dynamics. The effectiveness of the proposed approach is evaluated and tested using a biped robot with fourteen degrees of freedom.

2. ZERO MOMENT POINT CONCEPT

The biped locomotion process is generally divided into single and double support stages. In single support, the biped robot's weight rests on only one leg, while in double support it rests with the help of both legs. Additionally, these stages are usually analyzed in two kinematic planes: Sagittal and lateral (Vukobratovic et al., 1990; Winter, 1990). The sagittal plane splits the robot's body into the left and right halves, while the lateral plane splits the robot into the front and rear halves. It is known that for stable gaits the robot's kinematics in the sagittal plane are more important than those in the lateral plane, since the sagittal plane is parallel to locomotion process. However, it has been demonstrated that the lateral plane does also play a fundamental role in robot stabilization (Yamaguchi et al., 1993).

The most important task during biped locomotion is to preserve posture and gait stability. One of the most effective tools for biped posture stabilization analysis is provided by the zero moment point (ZMP) concept (Vukobratovic and Stokic, 1975). This method is based on the fact that single support quasi-static biped robot stability is achieved by "*ensuring the foot's whole area, and not only the edge, is in contact with the ground*" (Vukobratovic and Borovac, 2004) (Figure 1).

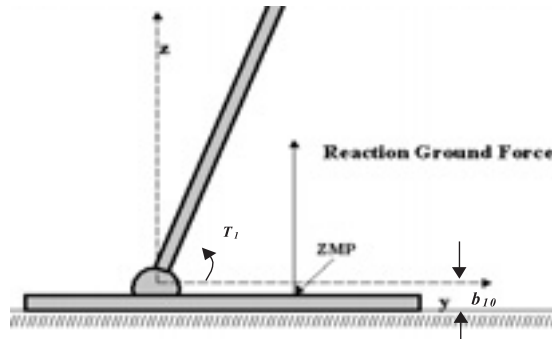


Figure 1. The ZMP concept.

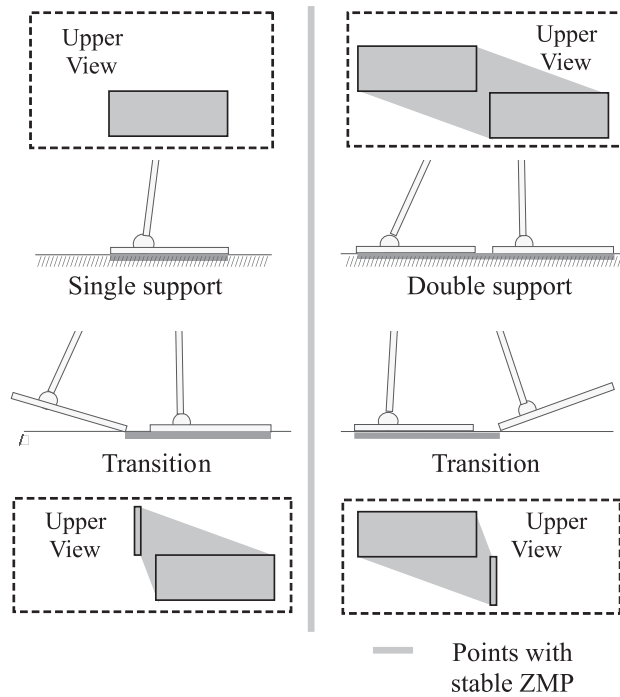


Figure 2. ZMP stability criteria from foot support area.

The ZMP is defined as the point where the ground reaction force is exactly counteracting the total moment generated by inertial and gravitational effects. Some researchers (Takanishi et al., 1989; Yamaguchi et al., 1993; Hirai et al., 1998; Fujimoto et al., 1998; Hirai, 1999) have suggested the following ZMP stability criteria: *“The Zero Moment Point of a biped robot must be constrained within the convex hull of foot support area to ensure stability of the foot ground contact. This convex hull is the smallest convex set containing foot or feet ground contact points”* (see Figure 2).

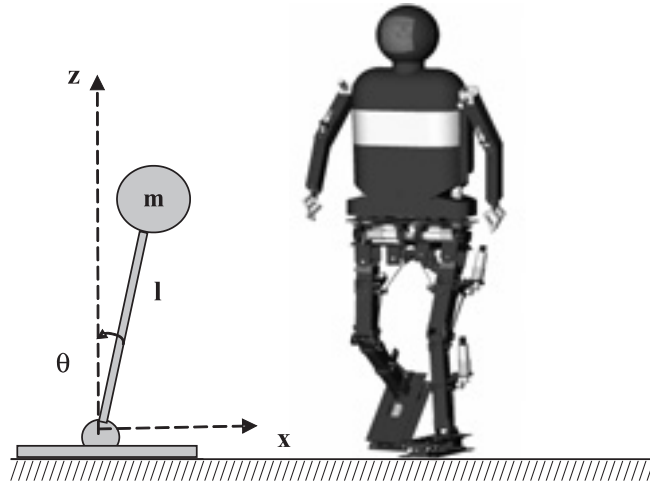


Figure 3. Inverted pendulum model.

3. BIPED ROBOT GAIT STABILIZATION

As was mentioned before, the ZMP is a very useful tool in synthesizing appropriate gaits for walking locomotion of bipedal robots (Takanishi et al., 1989; Yamaguchi et al., 1993; Hirai et al., 1998; Fujimoto et al., 1998). Most of these previous works can be separated into two categories: Offline motion generation and real-time motion generation (Sugihara et al., 2002). In the first category, biped robot joint controllers must follow pre-calculated ZMP stable trajectories, while in the second, trajectories are calculated online in accordance with ZMP stability and the pre-provided objectives of the robot's motion.

However, due to the fact that both motion generation approaches consider motors as ideal torque generators and the robot's mechanical structures as ideal rigid body linkages (in order to avoid high computational load), dynamics like joint backlashes, actuator saturation, and some structural vibration modes, any of which could compromise robot gait stability, are left unmodelled. This lack of gait robustness could be improved if the ZMP location is directly fed back into the biped robot's motion generator with the help of the ZMP sensor array (Caballero et al, 2004).

Furthermore, the full ZMP mathematical model is too complex to be employed in real time trajectory planning, and such complexity cause difficulties to use it in direct feedback ZMP based control systems. This drawback is due to the fact that there exists a nonlinear coupling between the robot dynamics, ground reaction force and ZMP (Takanishi et al., 1989; Yamaguchi et al., 1993). One way to overcome the problem of ZMP model complexity is to use reduced order models (Hemami, 1976). These model simplifications are based on the fact that most human movements support the principle of conservation of total angular momentum about the body's center-of-mass (Popovic et al., 2004a,b).

Previous works (Hemami et al., 1973) have suggested that a footed inverted pendulum (Figure 3) can be used to approximate a full biped system. This reduced order model approximates full biped dynamics using the following system equations:

Dynamical equations:

$$m\ddot{x}_c = f_x \quad (1)$$

$$m\ddot{y}_c = f_y \quad (2)$$

$$m(\ddot{z}_c + g) = f_z \quad (3)$$

ZMP constraints:

$$(ZMP_x - x_c) f_z + (z_c - ZMP_z) f_x = 0 \quad (4)$$

$$(ZMP_y - x_y) f_z + (z_c - ZMP_z) f_y = 0. \quad (5)$$

Where m is the total mass of the robot, x_c , y_c and z_c are the coordinates of the robot's center of mass, f_x , f_y and f_z comprise the reaction ground force, ZMP_x , ZMP_y and ZMP_z are the ZMP ground position and g is the acceleration due to gravity. Now, after manipulating equations (1) to (5), the relationship between the ZMP and the robot's center of mass can be expressed as follows:

$$ZMP_x = \frac{x_c m (\ddot{z}_c + g) - (z_c - ZMP_z) m \ddot{x}_c}{m (\ddot{z}_c + g)} = x_c - \alpha(t) \ddot{x}_c \quad (6)$$

$$ZMP_y = \frac{y_c m (\ddot{z}_c + g) - (z_c - ZMP_z) m \ddot{y}_c}{m (\ddot{z}_c + g)} = y_c - \alpha(t) \ddot{y}_c \quad (7)$$

$$\alpha(t) = \frac{(z_c - ZMP_z)}{(\ddot{z}_c + g)}. \quad (8)$$

This last expression can provide further insight into the physical meaning of $\alpha(t)$. If in equation (8) $\frac{\ddot{z}_c}{g} \approx 0$, indicating that the vertical acceleration of the robot is much smaller than the acceleration due to gravity (which is the case for quasi-static locomotion), then $\alpha(t)$ can be considered constant and approximated by $\alpha \approx \frac{(z_c - ZMP_z)}{g} = \frac{1}{\omega_c^2}$, where ω_c can be interpreted as the natural frequency of the equivalent pendulum.

However, the aim of this research is not only to fit the biped robot to an inverted pendulum model, but also to obtain an uncertainty model, in order to consider inverted pendulum approximation errors and nonlinear effects. This kind of modeling will help to accomplish real time modeling in direct feedback ZMP based control systems without losing gait robustness.

4. FREQUENCY RESPONSE MODELING

The relationship between the ZMP and biped robot motion in equations (6) to (8) is not only nonlinear, but also dynamically coupled. This complexity can be handled by obtaining a

linearization model around a center of mass operation point $(\bar{x}_c, \bar{y}_c, \bar{z}_c)$, allowing equations (6), (7) and (8) to be written as:

$$ZMP_x = \overline{ZMP}_x + ZMP_{\Delta x} \quad (9)$$

$$\overline{ZMP}_x = \bar{x}_c \quad (10)$$

$$ZMP_{\Delta x} = x_{\Delta c} - \bar{\alpha}\ddot{x}_{\Delta c} = x_{\Delta c} - \frac{1}{\omega_c^2}\ddot{x}_{\Delta c} \quad (11)$$

$$ZMP_y = \overline{ZMP}_y + ZMP_{\Delta y} \quad (12)$$

$$\overline{ZMP}_y = \bar{y}_c \quad (13)$$

$$ZMP_{\Delta y} = y_{\Delta c} - \bar{\alpha}\ddot{y}_{\Delta c} = y_{\Delta c} - \frac{1}{\omega_c^2}\ddot{y}_{\Delta c} \quad (14)$$

$$\bar{\alpha} = \frac{(\bar{z}_c - ZMP_z)}{g} = \frac{1}{\omega_c^2}. \quad (15)$$

Since $\bar{\alpha} > 0$ the small signal model (equations (11) and (14)) clearly introduces one RHPZ (right half plane zero) in the root locus plane. Such a system is known in control system literature as a non-minimum phase and usually defines an important limitation in a closed loop regime (Skogestad and Postlethwaite, 1996).

One of the simplest methods utilized in system modeling is the frequency response technique. In order to obtain a nominal biped robot frequency response model for the ZMP (taking account of its characteristic uncertainty), the biped robot's center of mass is excited with a variable frequency sinusoidal signal at several operating points:

$$x_{\Delta c} = x_0 \sin(\omega t) \quad (16)$$

$$y_{\Delta c} = y_0 \sin(\omega t). \quad (17)$$

These input oscillations (of varying frequency) generate other output oscillations that can be analyzed with the help of the ZMP measurement system (Figure 4). Another important advantage of this method is the fact that after equations (16) and (17) are applied in (11) and (14), $ZMP_{\Delta x}$ and $ZMP_{\Delta y}$ are in phase with the inputs $x_{\Delta c}$ and $y_{\Delta c}$, respectively. It is then possible to write:

$$ZMP_{\Delta x} = x_{0ZMP} \sin(\omega t) \quad (18)$$

$$ZMP_{\Delta y} = y_{0ZMP} \sin(\omega t). \quad (19)$$

Reducing the problem to an $\bar{\alpha}$ simple estimation problem for each operation point:

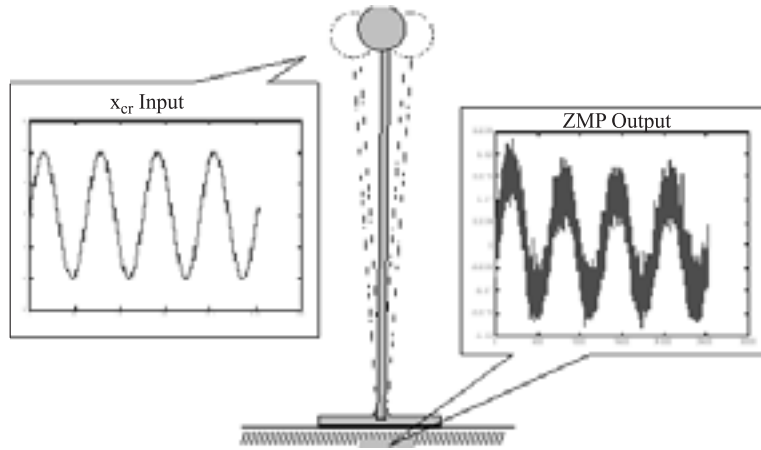


Figure 4. Frequency response method.

$$x_{0zmp} = (1 + \bar{a}\omega^2) x_0 = \left(1 + \frac{\omega^2}{\omega_c^2}\right) x_0 \quad (20)$$

$$y_{0zmp} = (1 + \bar{a}\omega^2) y_0 = \left(1 + \frac{\omega^2}{\omega_c^2}\right) y_0. \quad (21)$$

However, perfect tracking of the center of mass reference ($x_c(t) \rightarrow x_{cr}(t)$, $y_c(t) \rightarrow y_{cr}(t)$) is not always feasible. These tracking errors are related to uncertainties in robot mass distribution, actuator saturation, joint backlashes, structure flexibilities and other unmodelled dynamics. Nevertheless, this complex relationship between the actual and reference center of mass could be modelled using a “harmonic balance” method (Caballero et al., 2002). This technique is designed to obtain an average transfer function (analyzing the first harmonic term) and associated uncertainty function. Hence, for low frequency signals, the average ZMP model becomes:

$$ZMP_{\Delta x} = a_x x_{\Delta cr} - b_x \ddot{x}_{\Delta cr} \quad (22)$$

$$ZMP_{\Delta y} = a_y y_{\Delta cr} - b_y \ddot{y}_{\Delta cr}. \quad (23)$$

Where a_x , b_x , a_y and b_y account for the unmodelled dynamic effects.

The nonlinear ZMP model can now be analyzed in three sections (Figure 5). The first section matches biped robot dynamics to equivalent inverted pendulum dynamics. In this section, not only saturation effects in robot acceleration, but also the averaged harmonic effects of the unmodelled dynamics are considered. The second stage models the uncertainty of the inverted pendulum model, including nonlinear effects. The last stage acts like a low pass filter, defining the effective system cut-off frequency due to the effects of tracking the center of mass reference signals (x_{cr} and y_{cr}).

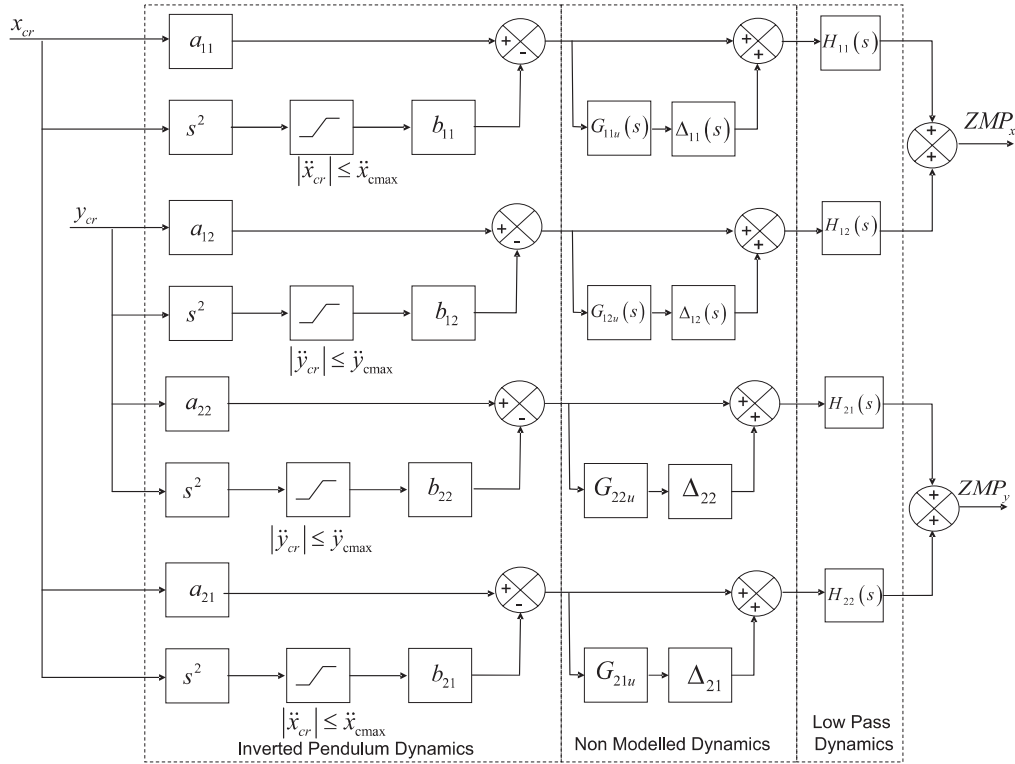


Figure 5. ZMP frequency domain model.

5. ZERO MOMENT POINT MODELING ALGORITHM

The harmonic balance based algorithm proposed is designed to obtain the parameters a_{ij} and b_{ij} , uncertainty transfer function G_{ij} , and system cut-off frequency H_{ij} . The first step of this algorithm consists of building up a ZMP database for small oscillation inputs in n_o operating points. In this step, transient regimes are eliminated and only the steady state is recorded for n_k sampling points, n_l amplitude and n_f frequency harmonic input signals (Figure 6).

The second step is designed to fit the biped robot to inverted pendulum dynamics. At this stage, a windowing algorithm is applied to the gathered data and then a fast Fourier transform (FFT) algorithm is applied in order to obtain an initial estimate of the amplitude and phase of the ZMP transfer function. Next, a statistical nonlinear regression algorithm (using the amplitude and phase provided by the FFT as an initial estimate) is applied in order to improve the input-output frequency model. Finally, a new nonlinear regression is applied in order to fit ZMP biped model with:

$$G_{invp_ij}(s)|_{s=j\omega} = a_{ij} - b_{ij}s^2 = a_{ij} + b_{ij}\omega^2 \tag{24}$$

for x_{cr} , and y_{cr} inputs and ZMP_x and ZMP_y outputs (Figure 7).

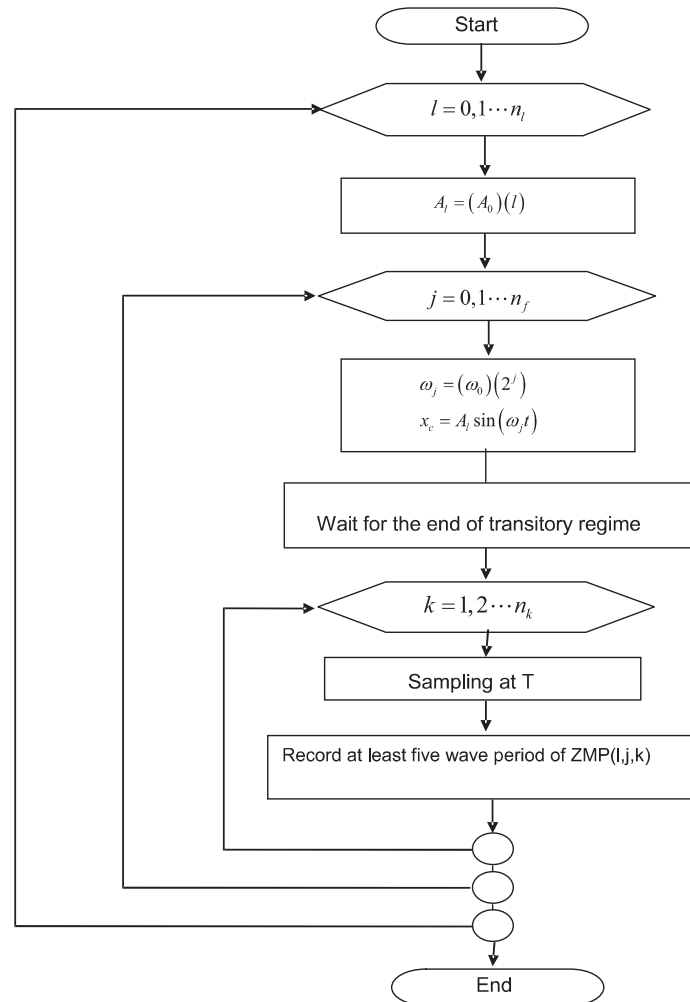


Figure 6. Algorithm for building a database relating ZMP values to the amplitude and frequency of the harmonic input signals.

The third step is focused on estimating the effective system bandwidth due to the effects of tracking. It has been demonstrated that this cut-off frequency can be approximated from servo controller bandwidth (Caballero et al., 2004).

The last step consists of building up an uncertainty transfer function database (see Figure 8). Here, the influence of nonlinear effects can be considered using harmonic balance, not only because it has the low-pass filter properties of the third section, but also because of the time invariant properties of the system. This uncertainty database will be very useful for designing robust direct ZMP feedback controllers, which assist in attenuating the uncertainty transfer function effects.

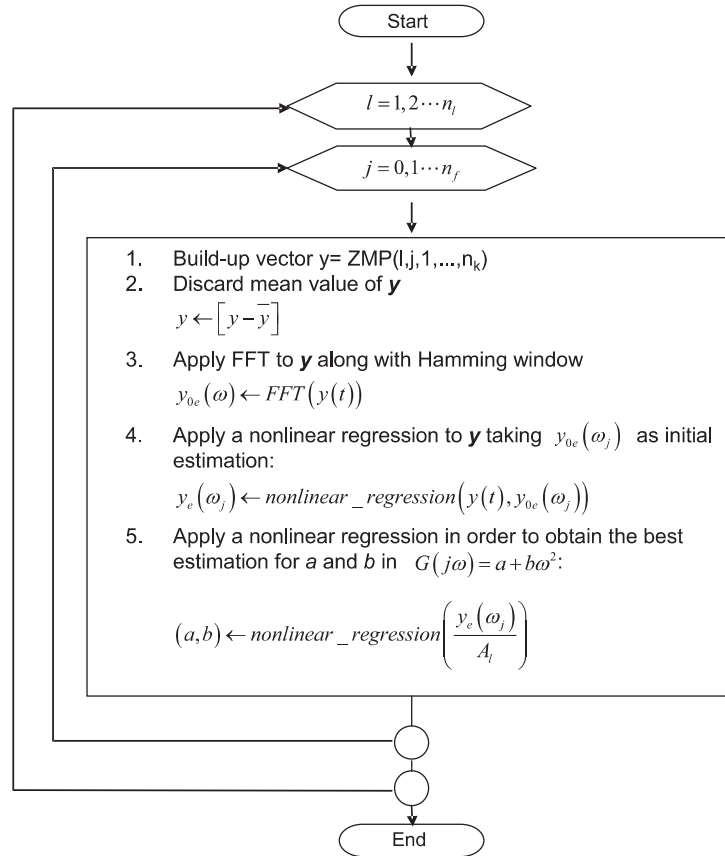


Figure 7. Algorithm used for fitting the biped robot to inverted pendulum dynamics.

6. EXPERIMENTAL RESULTS

The experimental set-up consists of a biped robot with 14 degrees of freedom (SILO2) (Figure 9), with four force sensors in each foot in order to measure its ZMP. Experiments are intended not only to determine the robot's equivalent inverted pendulum model, but also to assist with the development of a preliminary ZMP direct feedback for robot stabilization in double support. Displacement of the biped robot's center of mass is achieved with the help of trunk mass motion. This trunk which mass represents about 17% of the overall SILO2 48 kg and it provides the last two degrees of freedom to the robot.

6.1. Building up a ZMP Database

The first part of the experiment focuses on tracking the trajectories of the center of mass oscillations in the lateral (x axis) and sagittal (y axis) planes. This effect can be approximated if trunk motion is tracked with sinusoidal profiles:

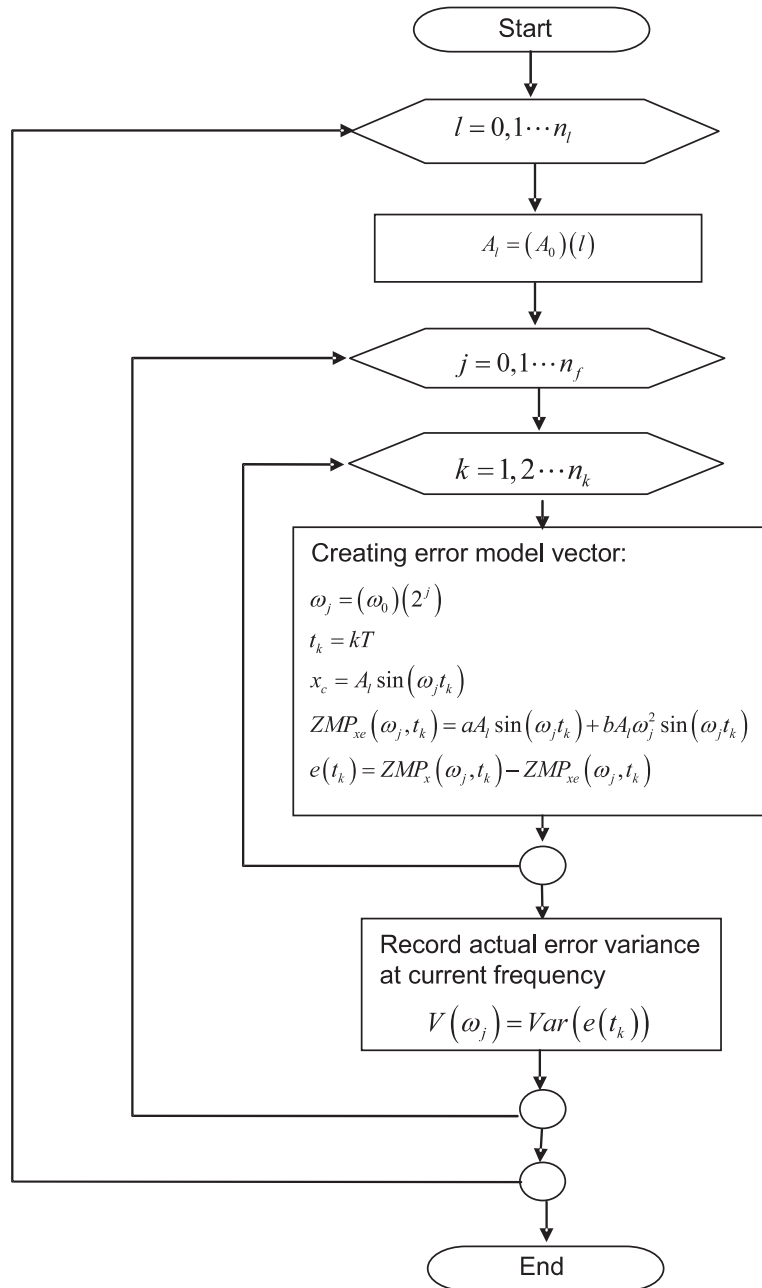


Figure 8. Algorithm used for determining the uncertainty dynamics.

$$\begin{aligned}
 x_{\Delta cr}(t) &\approx \left(\frac{m_t}{m_r}\right) l_t \theta_{\Delta lr}(t) \\
 \theta_{\Delta lr}(t) &= \theta_0 \sin(\omega t)
 \end{aligned} \tag{25}$$

$$\begin{aligned}
 y_{\Delta cr}(t) &\approx \left(\frac{m_t}{m_r}\right) l_t \theta_{\Delta sr}(t) \\
 \theta_{\Delta sr}(t) &= \theta_0 \sin(\omega t)
 \end{aligned} \tag{26}$$

where $x_{\Delta cr}(t)$ and $y_{\Delta cr}(t)$ correspond to small displacements of the robot's center of mass reference around the operation point, $\theta_{\Delta l}(t)$ and $\theta_{\Delta s}(t)$ correspond to small angular displacements of reference trunk angles, m_t is the trunk mass, m_r is the total biped robot mass and l_t is the trunk length (see Figures 9 and 10; ZMP and time are in meters and seconds, respectively).

6.2. Fitting the biped robot to inverted pendulum dynamics.

Once the ZMP database has been recorded, an FFT and harmonic nonlinear regression are applied in order to obtain the best-match a and b parameters. The experimental results corroborate the inverted pendulum approximation in the lateral and sagittal planes (see the Bode diagrams in Figures 11 and 12). Also, they demonstrate that there is some dynamical coupling between the lateral and sagittal plane dynamics (see Bode diagrams in Figures 13 and 14); the following a_{ij} and b_{ij} parameters were obtained:

$$\begin{aligned}
 a_{11} &= 0.8293; & a_{12} &= 0.07455; & a_{21} &= 0.1895; & a_{22} &= 1.245 \\
 b_{11} &= 0.2767; & b_{12} &= 0.005428; & b_{21} &= 0.09979; & b_{22} &= 0.1012.
 \end{aligned}$$

6.3. Effective System Bandwidth Estimation

Some preliminary experiments have demonstrated the low pass characteristics of ZMP systems at high frequencies (Caballero et al, 2004). These low pass characteristics are highly dependent on the system's maximum acceleration. This saturation effect limits zero moment point and center of gravity differences at higher frequencies. Also, there is a limit in tracking high frequency reference signals, due to the fact that servo controllers act as low pass filters. Some previous experiments have demonstrated that SILO2 servo controllers have a cut-off frequency of between 15 and 30 radians per second. This effect is approximated by a second order transfer function (errors in this model are considered as part of the system uncertainty):

$$H_{11} = H_{12} = H_{21} = H_{22} = \frac{\omega_n^2}{s^2 + 2\zeta\omega_n s + \omega_n^2} = \frac{900}{s^2 + 60s + 900}.$$

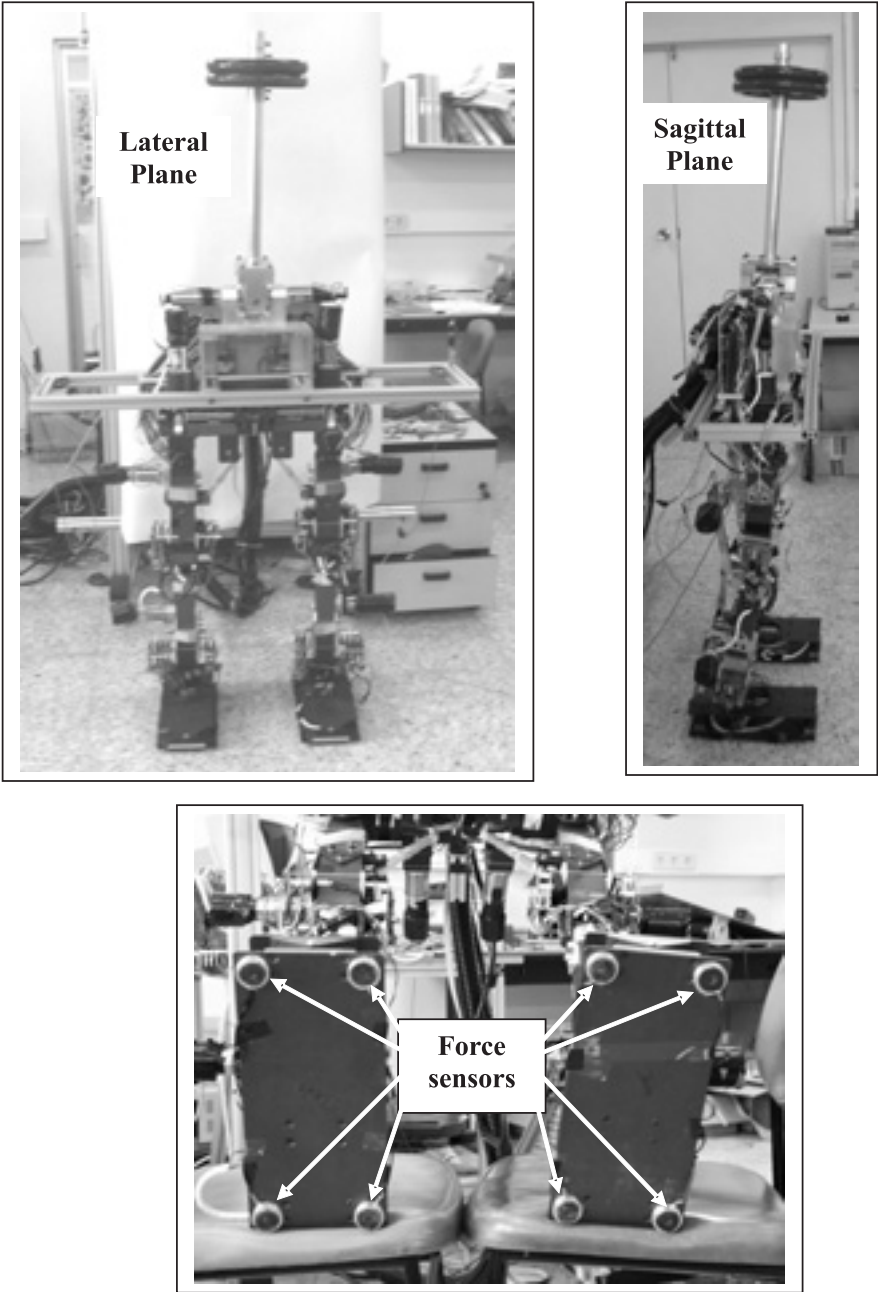


Figure 9. SILO2 biped robot.

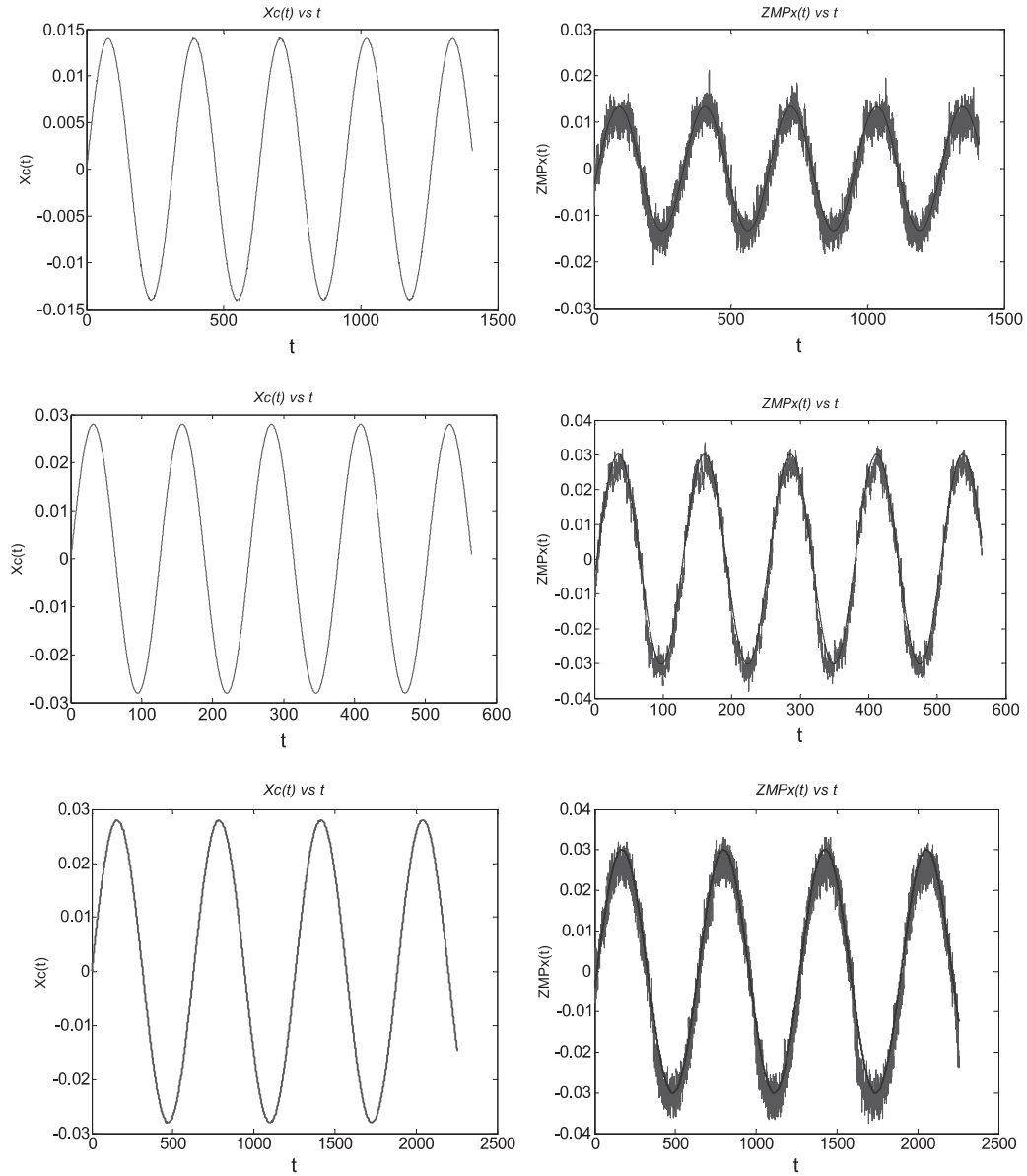


Figure 10. $ZMP_x(t)$ output for different $x_c(t)$ harmonic inputs.

6.4. System Uncertainty Estimation

In order to consider modeling errors occurring in previous steps, the proposed nominal model for each frequency is compared with the recorded database and the error between the nominal and real models is recorded for each frequency. As a result, the standard deviation in function of frequency acts like a high pass filter (see the Bode diagrams in Figure 15). After this, it is

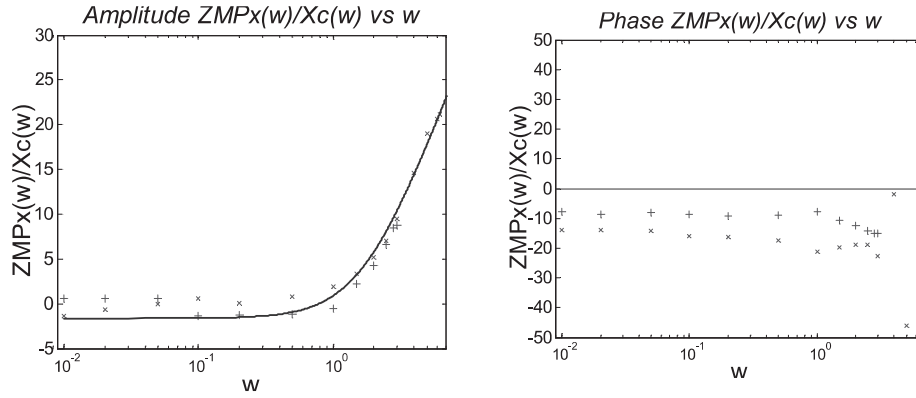


Figure 11. Bode diagrams for $ZMP_x(w)/X_c(w)$ output against w .

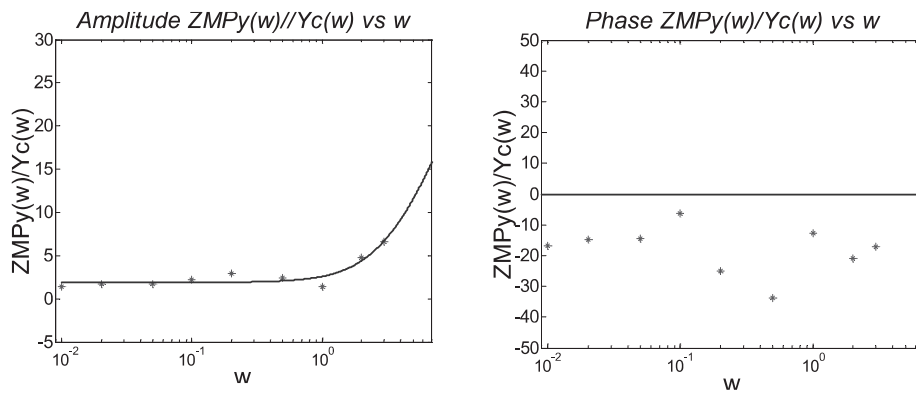


Figure 12. Bode diagrams for $ZMP_y(w)/Y_c(w)$ output against w .

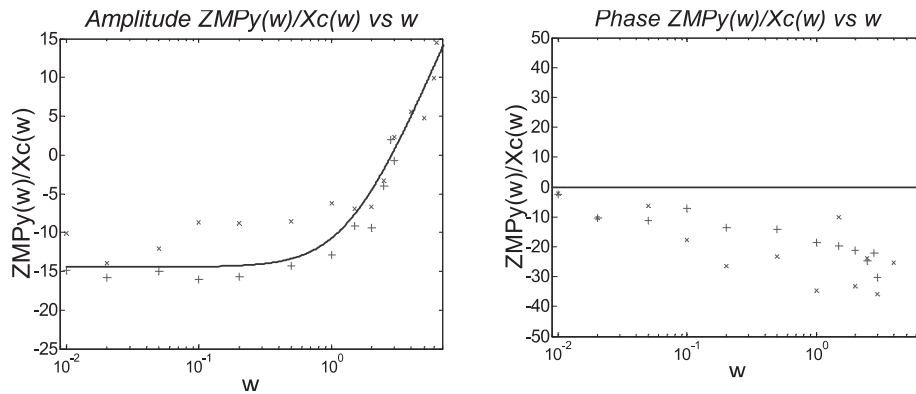


Figure 13. Bode diagrams for dynamical coupling $ZMP_y(w)/X_c(w)$.

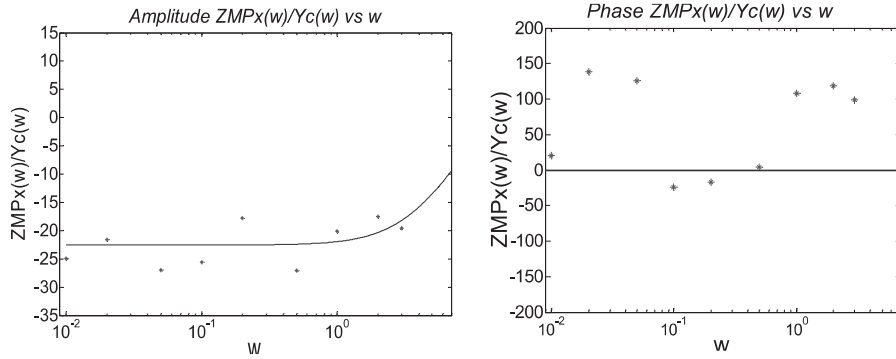


Figure 14. Bode diagrams for dynamical coupling $ZMP_x(w)/Y_c(w)$.

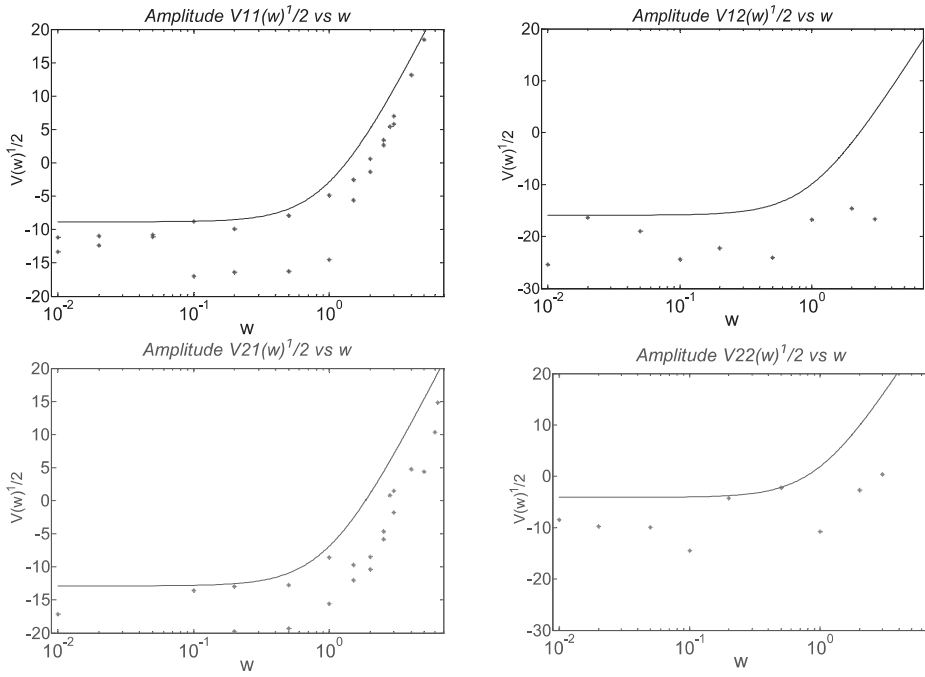


Figure 15. Bode diagrams for additive uncertainties.

possible to model multiplicative uncertainties as proposed in the model in Figure 5 instead of using additive uncertainties. As a result of this conversion, the following multiplicative uncertainty transfer functions (see Bode diagrams in Figure 16) are obtained:

$$G_{11u} = 4 \frac{s+1}{s+10}; \quad G_{12u} = 4 \frac{s+5}{s+20}; \quad G_{21u} = 7 \frac{s+1}{s+10}; \quad G_{22u} = \frac{s+0.1}{s+0.3}.$$

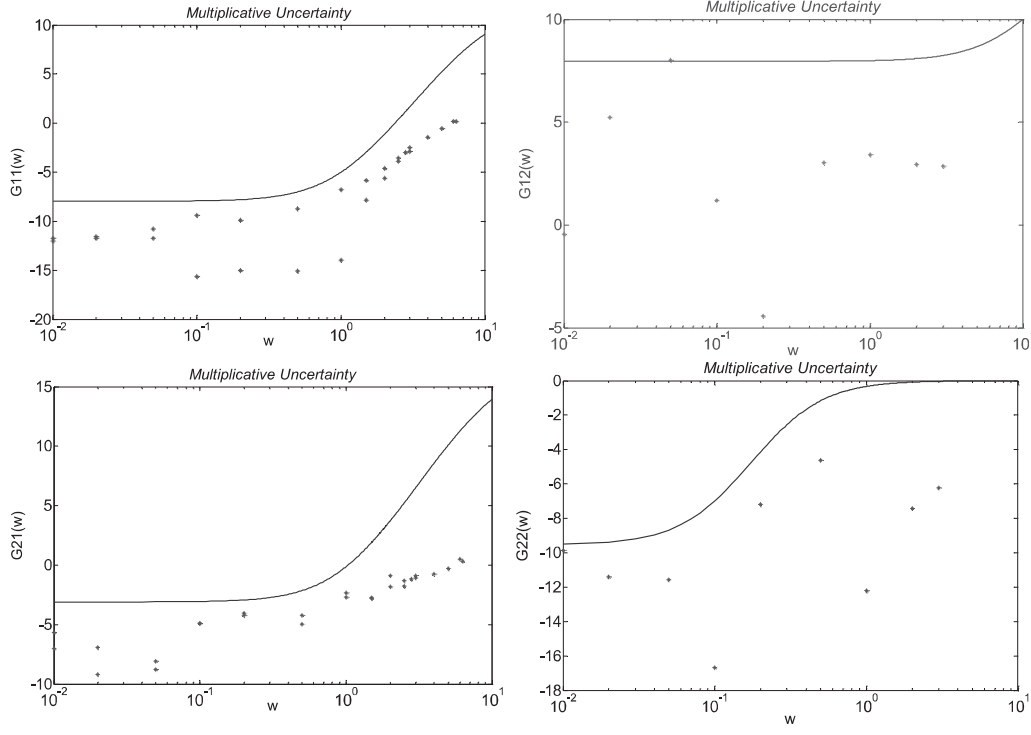


Figure 16. Bode diagrams for multiplicative uncertainties.

6.5. ZMP Small Signal Model

The ZMP dynamical model described in Figure 5 could be represented in Small Signal form (without acceleration saturation effect) by the equivalent multivariable system:

$$\begin{bmatrix} ZMP_x \\ ZMP_y \end{bmatrix} = G_{ZMP} \begin{bmatrix} x_{cr} \\ y_{cr} \end{bmatrix} .$$

Where

$$G_{ZMP} = 900 \begin{bmatrix} \left(\frac{0.8293-0.2767s^2}{s^2+60s+900} \right) \left(1 + 4 \frac{s+1}{s+10} \Delta_{11} (s) \right) \left(\frac{0.07455-0.005428s^2}{s^2+60s+900} \right) \left(1 + 4 \frac{s+5}{s+20} \Delta_{12} (s) \right) \\ \frac{0.1895-0.09979s^2}{s^2+60s+900} \left(1 + 7 \frac{s+1}{s+10} \Delta_{21} (s) \right) \left(\frac{1.245-0.1012s^2}{s^2+60s+900} \right) \left(1 + \frac{s+0.1}{s+0.3} \Delta_{22} (s) \right) \end{bmatrix}$$

$$\|\Delta_{11} (s)\| = \|\Delta_{12} (s)\| = \|\Delta_{21} (s)\| = \|\Delta_{22} (s)\| = 1$$

and although $G_{ZMP}(s)$ is stable and diagonal dominant, the presence of right half plane zeros in this system defines it as a non-minimum-phase dynamic system.

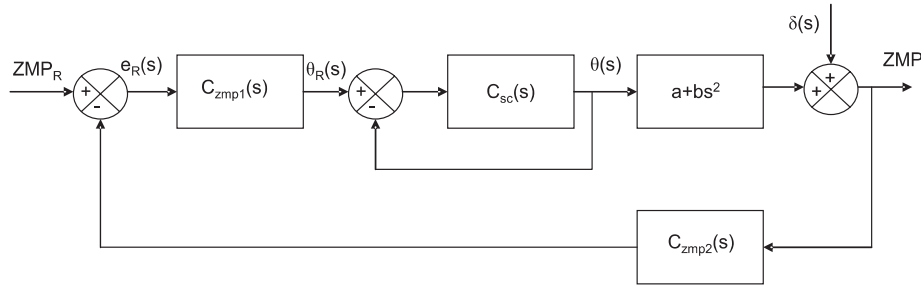


Figure 17. ZMP direct feedback controller.

6.6. Testing a ZMP Direct Feedback Controller

In order to test the effectiveness of the ZMP model, the SILO2 trunk reference trajectory was now directly controlled using ZMP direct feedback. As is shown in Figure 17, it is a two timescale cascade controller. The inner loop is a fast position servo controller loop, and the outer loop is a slower ZMP controller. The reference position of the servo controller is directly driven by the ZMP controller, but the ZMP controller reference is a pre-provided objective in robot motion.

The proposed ZMP nominal model defines a non-minimum-phase system, and it is well known that this type of dynamics imposes some restrictions on controller performance. In order to accomplish these restrictions the following controller is proposed:

$$C_{cZmp1}(s) = \frac{K_1}{s} \tag{28}$$

$$C_{cZmp2}(s) = \frac{K_2}{s + K_2}. \tag{29}$$

The proposed controller was tested with $K_1 = 0.014$; $K_2 = 0.2$. The experiment consisted of changing the ZMP reference from $ZMP_R = 0.12m$ to a new reference at $ZMP_R = 0.17m$ at $t = 0$. As it can be seen from Figures 18 to 20, it took about 20 seconds to reach the set point. Next, at time $t = 80$ seconds, a 4 kg mass was placed on one side (right) of the robot. The ZMP controller then compensated for the ZMP reference error, changing the biped robot's center of mass with the help of trunk motion. Figure 21 shows a photographic sequence of the experiment.

This last experiment reveals the importance of ZMP modeling in the frequency domain. The robustness of the frequency domain model guarantees the robustness of the proposed controller with respect to several operating variables.

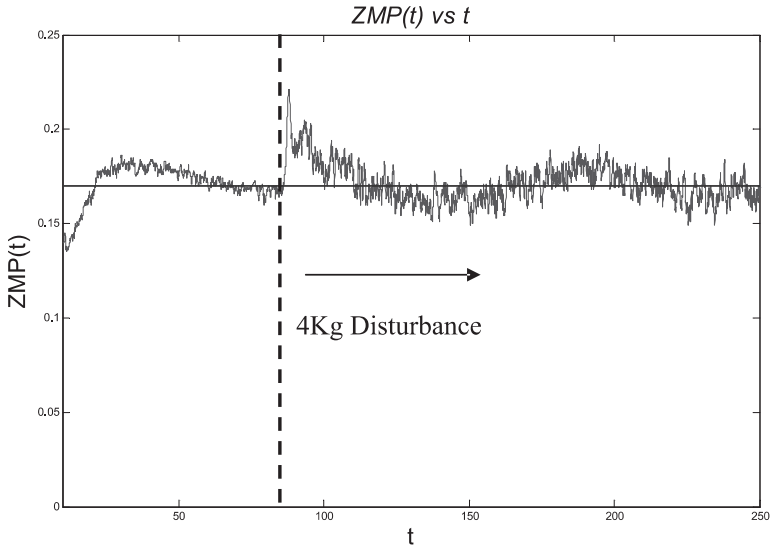


Figure 18. ZMP regulation with direct feedback. Units of ZMP and time are meters and seconds respectively.

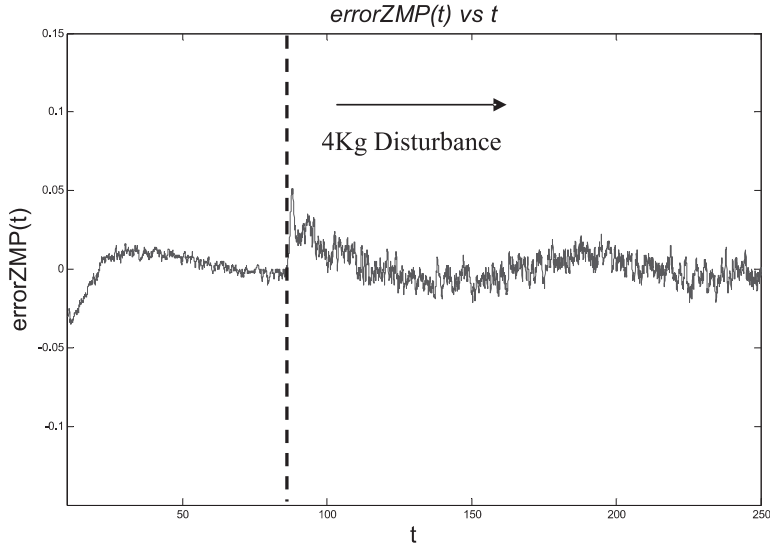


Figure 19. ZMP error regulation with direct feedback. Units of ZMP and time are meters and seconds respectively.

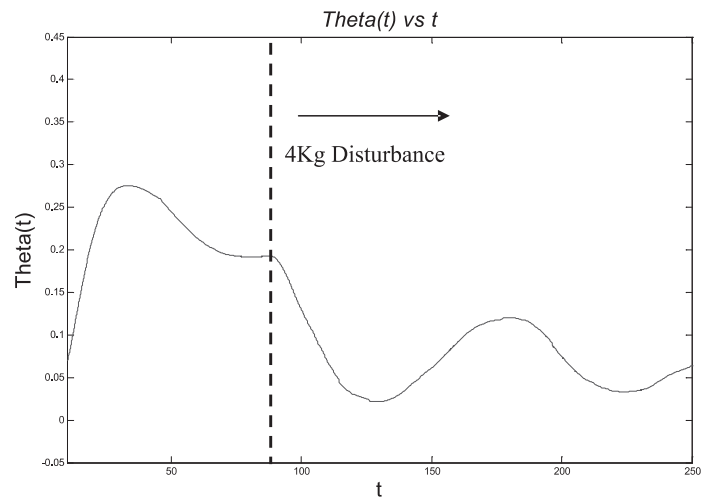


Figure 20. Trunk motion to accomplish ZMP regulation with direct feedback. Units of theta and time are radians and seconds respectively.

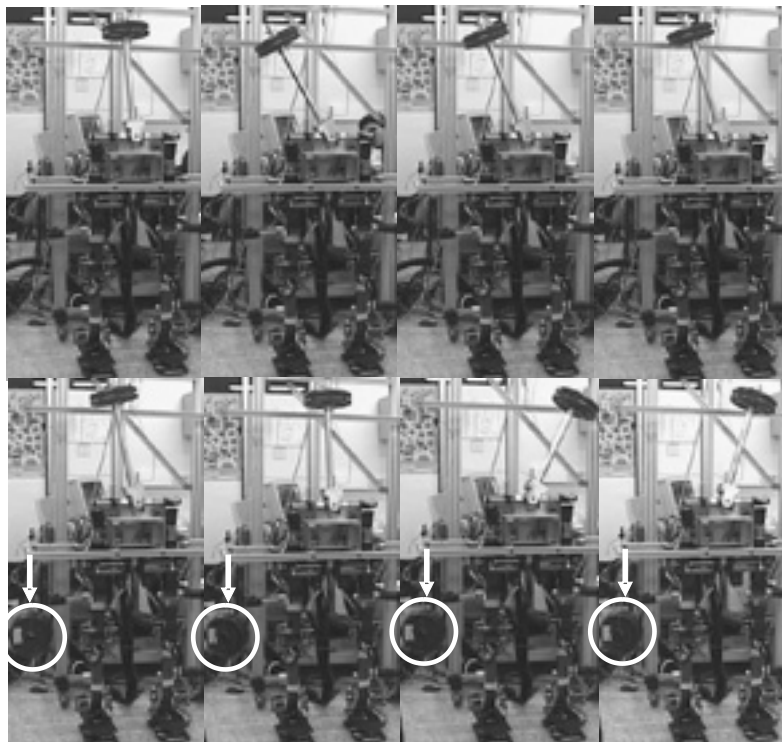


Figure 21. Experimental results for the ZMP direct feedback controller.

7. CONCLUSION

The proposed frequency domain modeling methodology has been successfully applied in double support to a biped robot with 14 degrees of freedom. Although the $G_{ZMP}(s)$ transfer function is stable and diagonal dominant, some coupling exists between the lateral and sagittal planes. Also, the inverted pendulum dynamic places two RHPZs (one each for the lateral and the sagittal planes) defining a non-minimum-phase dynamic for the ZMP. The actual position of these RHPZs is different for the lateral and sagittal planes. This difference can be explained by backlashes and mechanical structure differences in the planes. Also, the experiments have confirmed the time invariant and low pass filter properties of the ZMP model obtained. Finally, the proposed ZMP frequency domain methodology has been very useful not only in analyzing ZMP dynamics but also in designing a ZMP direct feedback controller.

This experiment was performed in double support; the same algorithm could be applied in order to obtain a set of single support models about different operation points. Finally, this type of frequency domain model will be very useful in synthesizing one or more robust controllers for ZMP direct feedback.

Acknowledgments. This research has been partially funded by Consejería de Educación of Comunidad de Madrid, under grant RoboCity2030 S-0505/DPI/0176. Dr. Caballero acknowledges the support received from Universidad Tecnológica de Panamá.

REFERENCES

- Armada, M. and González de Santos, P., 1997, "Climbing, walking and intervention robots," *Industrial Robot* **24**(2), 158–163.
- Armada, M., González de Santos, P., Jiménez, M. A., and Prieto, M., 2003, "Application of CLAWAR machines," *International Journal of Robotics Research* **22**(3–4), 251–264.
- Caballero, R., Akinfiyev, T., and Armada, M., 2002, "Robust cascade controller for ROBICAM biped robot: Preliminary experiments," in *Proceedings of the 5th International Conference of Climbing and Walking Robots*, Paris, France, pp. 147–154.
- Caballero, R., Akinfiyev, T., and Armada, M., 2004, "Robust cascade controller for nonlinearly actuated biped robots: Experimental evaluation," *International Journal of Robotics Research* **23**, 1011–1075.
- Fujimoto, Y., Obata, S., and Kawamura, A., 1998, "Robust biped walking with active interaction control between foot and ground," in *Proceedings of the 1998 IEEE International Conference on Robotics & Automation*, Leuven, Belgium, Vol. 3, pp. 2030–2035.
- Furushu, J. and Masubushi, M., 1986, "Control of a dynamical biped locomotion system for steady walking," *Journal of Dynamic Systems, Measurement, and Control* **108**, 111–118.
- Gienger, M., Löffler, K., and Pfeiffer, F., 1999, "Design and control of a biped walking and jogging robot," in *Proceedings of the 4th International Conference on Climbing and Walking Robots*, Portsmouth, UK, September, pp. 48–58.
- González de Santos, P., Armada, M., and Jiménez, M. A., 2000, "Ship building with ROWER," *IEEE Robotics and Automation Magazine* **7**(4), 35–43.
- González de Santos, P., Garcia, E., Estremera, J., and Armada, M., 2005, "Dylema: Using walking robots for landmine detection and location," *International Journal of System Science* **36**(9), 545–558.
- Goswami, A., 1999, "Postural stability of biped robots and the foot-rotation indicator (FRI) point," *International Journal of Robotic Research* **18**(6), 523–533.
- Hemami, H., 1976, "Reduced order models for biped locomotion," in *Proceedings of the 7th Pittsburgh Conference on Modeling and Simulation*, pp.270–276.
- Hemami, H., Weimer, F., and Koozekanani, S., 1973, "Some aspects of the inverted pendulum problem for modeling of locomotion systems," *IEEE Transactions on Automatic Control* **18**(16), 658–661.

- Hirai, K., 1999, "The Honda humanoid robot: Development and future perspective," *Industrial Robot* **26**(4), 260–266.
- Hirai, K., Hirose, M., Haikawa, Y., and Takenaka, T., 1998, "The development of Honda humanoid robot," in *Proceedings of IEEE International Conference on Robotics & Automation*, Leuven, Belgium, pp. 1321–1326.
- Medrano-Cerda, G. and Eldukhri, E., 1997, "Biped robot locomotion in sagittal plane," *Transactions of the Institute of Measurement and Control* **19**(1), 38–49.
- Mita, T., Yamagushi, T., Kashiwase, T., and Kawase, T., 1984, "Realization of a high speed biped using modern control theory," *International Journal of Control* **40**(1), 107–119.
- Pfeiffer, F., Löffler, K., and Gienger, M., 2000, "Design aspects of walking machines," in *Proceedings of the 3rd International Conference on Climbing and Walking Robots*, Madrid, pp. 17–38.
- Popovic, M. B., Hofmann, A. G., and Herr, H. M., 2004a, "Zero spin angular momentum control: Definition and applicability," in *Proceedings of the IEEE-RAS/RSJ International Conference on Humanoid Robots*, Los Angeles, CA.
- Popovic, M. B., Hofmann, A. G., and Herr, H. M., 2004b, "Angular momentum regulation during human walking: Biomechanics and control," in *Proceedings of the IEEE International Conference on Robotics and Automation*, New Orleans, LA, pp. 2405–2411.
- Skogestad, S. and Postlethwaite, I., 1996, *Multivariable Feedback Control*, John Wiley & Sons, Chichester, UK.
- Sugihara, T., Nakamura, Y., and Inoue, H., 2002, "Realtime humanoid motion generation through ZMP manipulation based on inverted pendulum control," in *Proceedings of the IEEE International Conference on Robotics & Automation*, Washington, DC, 11th–15th May, Vol. 2, pp. 1404–1409.
- Takanishi, A., Tochizawa, M., Taraki, H., and Kato, I., 1989, "Realization of dynamic biped walking stabilized with trunk motion under known external force," in *Proceedings of the International Conference on Advanced Robotics*, Columbus, OH, June.
- Virk, G. S., Muscato, G., Semerano, A., Armada, M., and Warren, H. A., 2004, "The CLAWAR project on mobile robotics," *Industrial Robot* **31**(2), 130–138.
- Vukobratovic, M. and Borovac, B., 2004, "Zero-moment point – thirty five years of its Life," *International Journal of Humanoid Robotics* **1**(1), 157–173.
- Vukobratovic, M. and Juricic, D., 1968, "Contribution to the synthesis of biped gait," in *Proceedings of the IFAC Symposium on Technical and Biological Problem on Control*, Erevan, USSR.
- Vukobratovic, M. and Stokic, D., 1975, "Dynamic control of unstable locomotion robots," *Mathematical Biosciences* **24**, 129–157.
- Vukobratovic, M., Borovac, B., Surla, D., and Stokic, D., 1990, *Biped Locomotion*, Springer-Verlag.
- Winter, D. A., 1990, *Biomechanics and Motor Control of Human Movement*, John Wiley & Sons, Chichester, UK.
- Yamaguchi, J., Takanishi, A., and Kato, I., 1993, "Development of a biped walking robot compensating for three-axis moment by trunk motion," in *Proceedings of the IEEE/RSJ International Conference on Intelligent Robots and Systems*, Yokohama, Japan, July, pp. 561–566.